Coupled Joint Registration and Co-segmentation for Indoor Rigid Object Sets

Siyu Hu*

1 Abstract

Keywords: Co-segmantion, Joint Registration

Concepts: •**Computing methodologies** → **Image manipulation;**
Computational photography;

1 Introduction

In many researches and applications of indoor scenes the data of segmented and even annotated 3D indoor scenes are required as either data base or training data (e.g.[Nan et al. 2012][Dema and Sari-Sarraf 2012][Fisher et al. 2012][Chen et al. 2014][Fisher et al. 2015]).

One way to build such data base is to interactively compose scenes from 3D shape models resulting in scenes with object segmentation and annotation naturally available, or to mannually segment and annotate existing scenes. This procedure can be tedious and time consuming, despite the efforts to improve the interaction experience(e.g.[Merrell et al. 2011][Xu et al. 2013]).

Another way is to automatically generate scenes from 3D shape models according to the input RGB or RGB-D images(e.g.[Liu et al. 2015][Chen et al. 2014]). In such methods, a retrieval procedure is usually needed and inevitably limit the result to a certain set of 3D models despite the actual 3D model in the input images. We prefer a approach that helps us build such data set directly from the captured data. One of the major gap between the required data set and available scene capturing framework(e.g.[Izadi et al. 2011]) is the general object level segmentation. We want to stress that a general object level segmentation problem should not be treated as an equivalence of multilabel classification problem since it is not limited to a certain set of objects. For 3D data, [Jia et al. 2015] used some simplified physical prior knowledge (i.e. the block based stability) to help acheiving the general object segmentation, while the work of [Xu et al. 2015] proposes a practical and rather complete framework to close the gap between the required data set and available scene capturing method. One of the observation in [Xu et al. 2015] is that the motion consistency of rigid object can serve as a strong evidence of general objectness. To exploit this fact, they employ a robot to do proactive push and use the movement tracking to verify and iteratively improve their object level segmentation result. Our work presented in this paper is trying to exploit the same observation from a different approach.

We intend to use the motion consistency that is naturally revealed by human activities along the time. Down to this approach, we are facing the choice of scanning scheme. One way is to record the change of the scene along with the human activities, another is to arrange a daily or even a once every half day sweep to only record the result of human activities but avoid the instant of human motion. The main challenge brought in by the second scheme is that we may not be able to solve the object correspondence by a local search due to the sparse sampling over time, but the very same challenge exists in the first scheme due to the exclusion caused by human bodies not to mention other additional process(e.g. tracking with severe oclussion) needed for human bodies. With the second scanning scheme, our original intention of building 3D scene data set from capturing naturally leads us to the problem of coupled joint registration and co-segmentation.

In this problem, registration and segmentaion are entangled in each other. On one hand the segmentation depends on the registration to connect the point clouds into series of rigid movement so that the object level segmentation can be done based on the motion consistency, on the other hand, the registration depends on the segmentation to break the problem into a series of rigid joint registration instead of a joint registration with non-coherent point drift(A pair of points is close to each other in one point set but their correspondent pair of points in another point set is far from each other, in other words, the point drift of this pair is non-coherent. This happens when this pair of points actually belong to different objects.) To model the problem, we employ a group of gaussian mixture models and each of these gaussian mixture models represents a potential objects. This modeling handles the entanglement of registration and segmentation in the way that

2 Related Work

2.1 Point Set Registration with GMM Representation

[Chui and Rangarajan 2000]
[Myronenko and Song 2010]
[Jian and Vemuri 2011]
Our work is most related to [Evangelidis et al. 2014]. We actually extend the formulation of [Evangelidis et al. 2014] to simultaneously handle joint registration and co-segmentation.

2.2 Functional Mapping

The coupled joint registration and co-segmentation problem comes with a latent problem of point-to-point correspondence problem. A series of work based on the functional maps representation advocated in [Ovsjanikov et al. 2012] have be done. In one of the most recent work [Maron et al. 2016], a convex relaxation technique was used to better approximate the global minimal for both rigid and non-rigid registration problem.

3 Method Overview

3.1 Problem Statement

Given a set of point clouds which record the same group of rigid indoor objects with different layout. We intend to samutaneously partition the point clouds into objects and align the points of same object to recover layouts for corresponding object. Figure **??** shows an example of input point clouds set.

3.2 Formulation

To formulate the relation between the unknown object set and the input point clouds. We come up with a generation model as follows:

---

*e-mail:sy891228@mail.ustc.edu.cn

$$P(v_{mi}) = \sum_{k=1}^{K_n} p_k N(\phi_{mn}(v_{mi})|x_k, \Sigma_k) \qquad (1)$$

which means, The observed point clouds are generated by N object model. Each object model is represented by a gaussian mixture model with K_n centroids. Our goal is to maximize the probability of the expected complete-data log-likelihood. The object function can be written as:

$$\Theta = \operatorname{argmax} \sum_Z P(Z|V, \Theta) \ln P(V, Z; \Theta) \qquad (2)$$

in which:

$$\Theta = \{\{p_k, x_k, \Sigma_k\}_{k=1}^{\sum K_n}, \{\phi_{mn}\}_{m=1,n=1}^{MN}\}$$

is the parameters of the generation model.

p_n is the prior probability that the point is generated by the n-th object.

p_k is the weight of the k-th Gaussian.

x_k is the center of the k-th Gaussian.

Σ_k is the standard deviation of the k-th Gaussian.

There are $\sum K_n$ Gaussian model in total and among them, K_n Gaussian models belongs to object n.

V is the M input point clouds.

v_{mi} is the i-th point of the m-th point cloud.

Z is a latent variable set defined as:

$$Z = \{z_{ij}|j = 1...M, i = 1...N_j\}$$

among which if $z_{ij} = k(k = 1... \sum K_n)$ assign the observation of $\phi_{mn}(v_{mi})$ to the k-th component of Gaussian mixture model. Such formulation can be seen as an extention of joint registration formulation in [Evangelidis et al. 2014], upon which we add several gaussian mixture model together to express a group of objects. By solving this new problem we simutaneously solve the object co-segmentation of given observation.

4 Algorithms and Implementation

4.1 Expectation Conditional Maximization

Assuming the observed point clouds $\{V_m\}$ are independent and identically distributed, we can then write the (2) as:

$$\varepsilon(\Theta|V, Z) = \sum_{m,i,k} \alpha_{mik}(\log p_k + \log P(\phi_{nm}(v_{mi})|z_{ji} = k; \Theta)) \qquad (3)$$

In which the $\alpha_{mik} = P(z_{mi} = k|v_{mi}; \Theta)$,

4.2 Initialization Techniques

A key advantage motivates our formulation is that the soft correspondence can be initialized more flexiblely comparing to the typical initialization techniques such as landmark point pairs in registration.

The result of Clustering:

$$P(B_{mj} \in C_n)$$

Soft Correspondence Initialization
Then the α is initialized as:

$$\alpha_{ijk} = P(B_{mj} \in C_n)$$

on the condition that:

$$v_{ij} \in B_{mj} \wedge x_k \in O_n$$

Algorithm 1 Joint Registration and Co-segmentation (JRCS)

Input:
$\{V_m\}$:Observed point clouds
$\{\alpha_{mik}^0\}$:Initial posterior probabilities
Output:
Θ^q:Final parameter set
1. $q \leftarrow 0$
2. **repeat**
3. CM-step-a: Use α_{mik}^q, x_k^{q-1} to estimate $\{R_{mn}^q\}$ and $\{t_{mn}^q\}$
4. CM-step-b: Use α_{mik}^q, $\{R_{mn}^q\}$ and $\{t_{mn}^q\}$ to estimate the Gaussian centers x_k^q
5. CM-step-c: Use α_{mik}^q, $\{R_{mn}^q\}$ and $\{t_{mn}^q\}$ to estimate the covariances Σ_k^q
6. CM-step-d: Use α_{mik}^q to estimate the priors p_k^q
7. E-step: Use Θ^{q-1} to estimate posterior probabilities. $\alpha_{mik}^q = P(z_{mi}|v_{mi}; \Theta^{q-1})$
8. $q \leftarrow q + 1$
9. **until** Convergence
10. **return** Θ^q

---

5 Experiments and Discussion

5.1 Experiment on Residue Correlation

Inputs:
We input a set of point clouds with the points consistently indexed respecting to their groundtruth correspondence, as shown in Figure 1.
Spectral Analysis:
In order to do spectral analysis on point clouds, we first build supervoxels with [Papon et al. 2013] on point cloud and then construct a graph laplacian as a matrix $L = (a_{ij})$ defined by:

$$a_{ij} = \begin{cases} -\alpha d_{ij} - (1-\alpha)c_{ij} & if\ i\ and\ j\ is\ an\ edge \\ \sum \alpha d_{ij} + (1-\alpha)c_{ij} & if\ i == j \\ 0 & otherwise \end{cases}$$

where $d_{ij} = \exp(\frac{-l_{ij}^2}{l_{mean}^2})$, l_{ij} is the length of the edge in the graph of supervoxels and l_{mean} is average length of all edges. c_{ij} is the function indicating convexity of the edge and is defined as:

$$c_{ij} = \begin{cases} 0 & if\ \theta_{dif} < -\epsilon \\ 1 & if\ \theta_{dif} > \epsilon \\ \frac{\theta_{dif}}{2\epsilon} + \frac{1}{2} & otherwise \end{cases}$$

where $\theta_{dif} = acos(< n_i, \frac{\overrightarrow{p_i p_j}}{||\overrightarrow{p_i p_j}||} >) - acos(< n_j, \frac{\overrightarrow{p_i p_j}}{||\overrightarrow{p_i p_j}||} >)$, in which the $\{n_i\}$ is the normal of supervoxels and $\{p_i\}$ is the center position of supervoxels. α is the weight between distance and convexity, for result in this paper we choose $\alpha = 0.5$.
Based on the laplacian matrix we can get its eigenfunctions $\{\phi_n\}_{n=0...N}$ respecting to the N smallest eigenvalues $\lambda_0...\lambda_N$.
We can design an indicating function that maps each of the points to a unique real value. If we make this function "continue" respecting to the order of index, it can be constructed as the one shown in Figure 2(a).
For each point clouds, we project the indicating function f onto the eigenfunctions by inner product and get coefficients: $\beta_n =< f, \phi_n >$. We choose M coefficients with largest absolute values to reconstruct the indicating function: $\hat{f} = \sum_{i=1}^{M} \beta_{n_m} \phi_{n_m}$ and the residue function of the reconstruction $r = f - \hat{f}$. The results of inputs(Figure 1) are shown in Figure 3. In Figure 3, the energy of
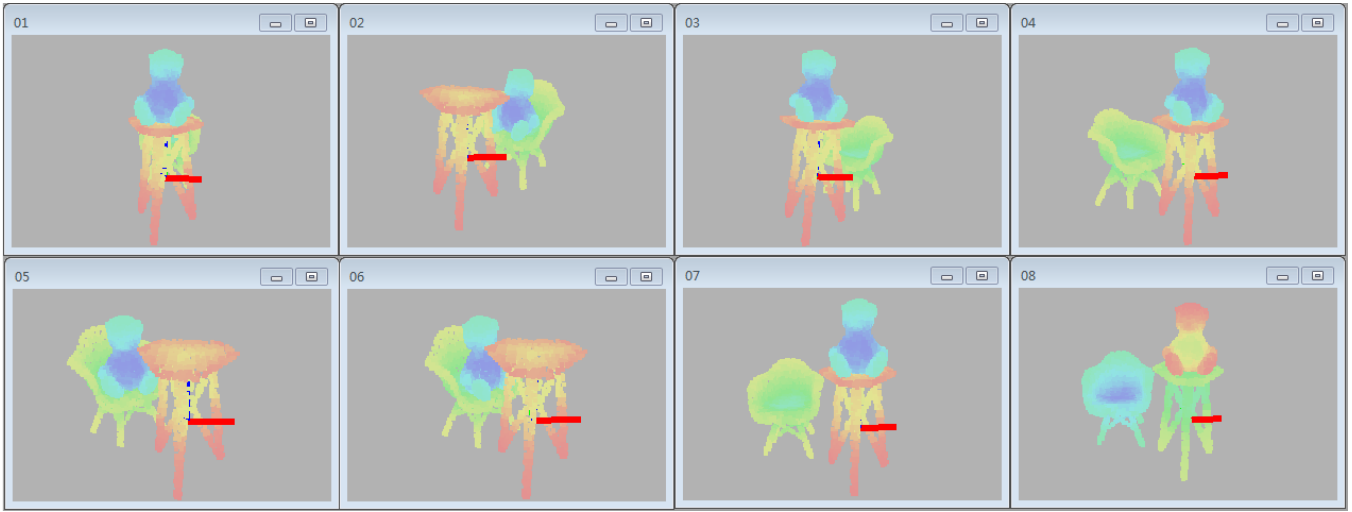
Figure 1: *Inputs of experiment on residue correlation: The points are colored by their index. From the color you should be able to see that: In frame 01 - 07, the points are indexed consistently respecting to object in order of table(1156 points), chair(1520 points), teddy(1351 points). In the frame 08, the points are indexed respecting to object in order of teddy, table, chair.*
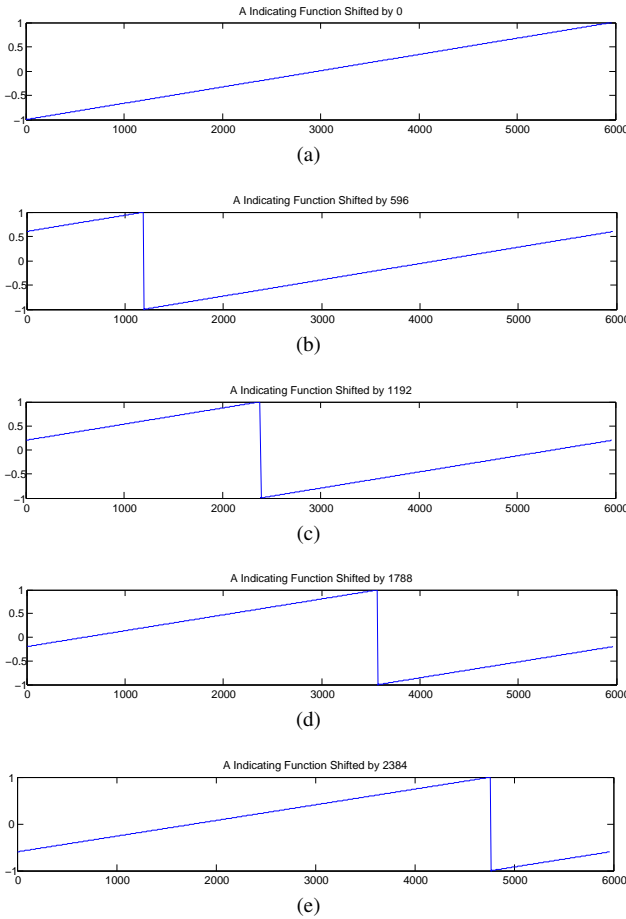
Figure 2: *Examples of indicating functions that is circularly shifted from the Figure 2(a) respecting to the index order.*
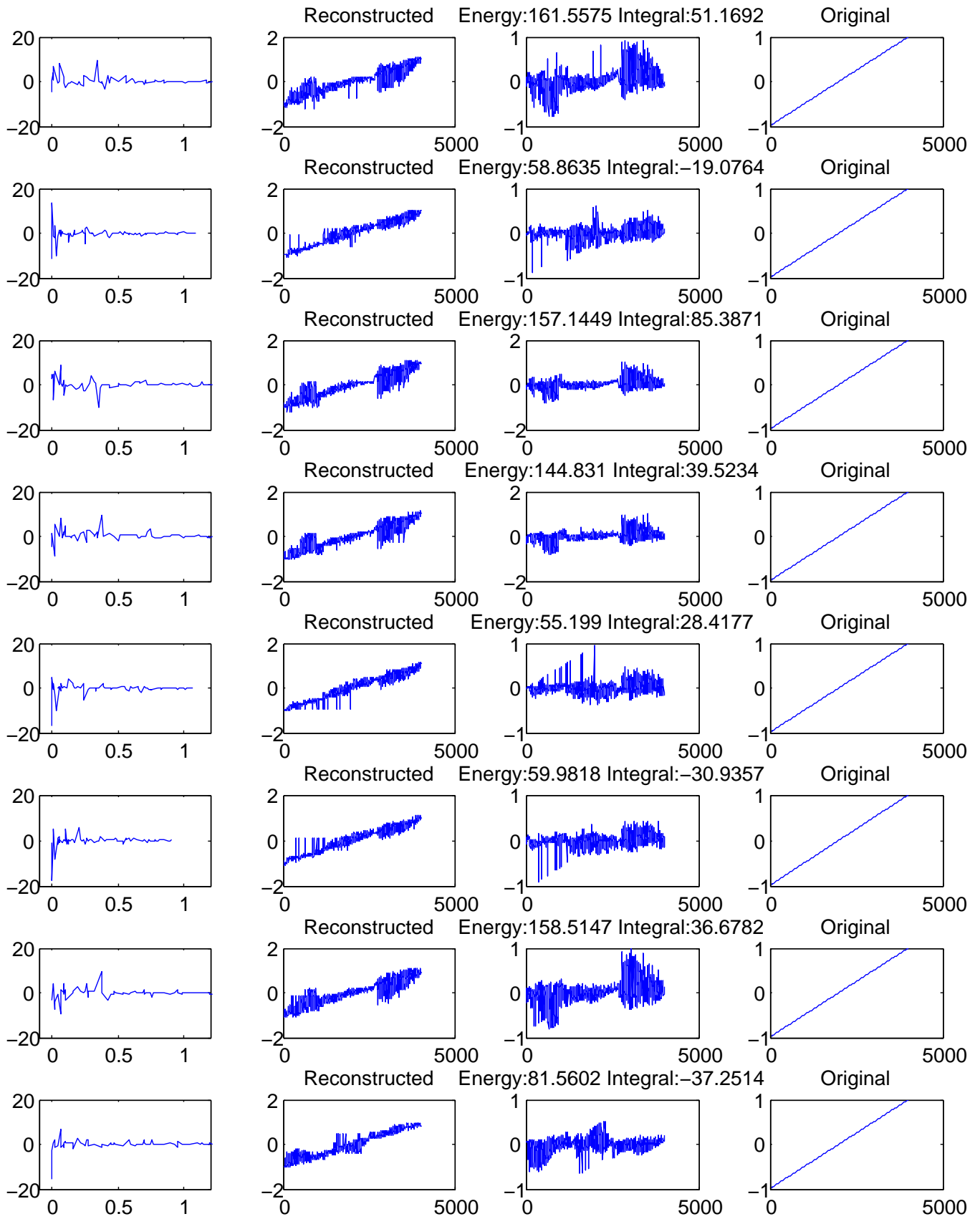
residue functions are calculated as $E = \sum r^2$.

We circularly shift the indicating functions as demonstrated in Figure 2. For each indicating function, we can calculate a residue energy. From Figure 4 we can see a clear similarity of the residue energy among the point clouds.

Acknowledgements

References

BOUAZIZ, S., TAGLIASACCHI, A., AND PAULY, M. 2013. Sparse iterative closest point. In *Proceedings of the Eleventh Eurographics/ACMSIGGRAPH Symposium on Geometry Processing*, Eurographics Association, Aire-la-Ville, Switzerland, Switzerland, SGP '13, 113–123.

BRONSTEIN, M. M., AND KOKKINOS, I. 2010. Scale-invariant heat kernel signatures for non-rigid shape recognition. In *Computer Vision and Pattern Recognition (CVPR), 2010 IEEE Conference on*, 1704–1711.

CHEN, K., LAI, Y.-K., WU, Y.-X., MARTIN, R., AND HU, S.-M. 2014. Automatic semantic modeling of indoor scenes from low-quality rgb-d data using contextual information. *ACM Trans. Graph. 33*, 6 (Nov.), 208:1–208:12.

CHUI, H., AND RANGARAJAN, A. 2000. A new algorithm for non-rigid point matching. In *Computer Vision and Pattern Recognition, 2000. Proceedings. IEEE Conference on*, vol. 2, 44–51 vol.2.

DEMA, M. A., AND SARI-SARRAF, H. 2012. 3d scene generation by learning from examples. In *Multimedia (ISM), 2012 IEEE International Symposium on*, 58–64.

EVANGELIDIS, G. D., KOUNADES-BASTIAN, D., HORAUD, R., AND PSARAKIS, E. Z. 2014. *A Generative Model for the Joint Registration of Multiple Point Sets*. Springer International Publishing, Cham, 109–122.

Figure 3: *Residue functions of indicating functions: Each row is correspondent to a frame shown in Figure 1. The first column is the spectrum of the indicating function. The Y axis is the value of coefficients and the X axis is the corresponding eigenvalue. The second column is the resconstructed indicating functions with M=30 absolute largest coefficients. The third column is the residue functions. The fourth column is the indicating functions.*
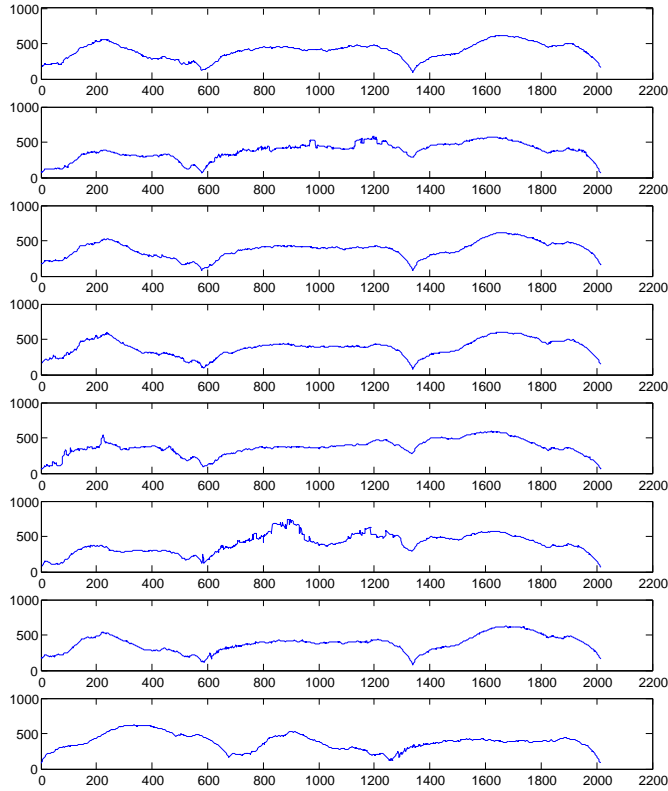
(a) When shift indicating functions with step = 2 we can get 2014 indicating functions and for each indicating function we can calculate a residue energy for reconstruction. We can see that though calculate independently on each point clouds, the residue energy have similar patterns.
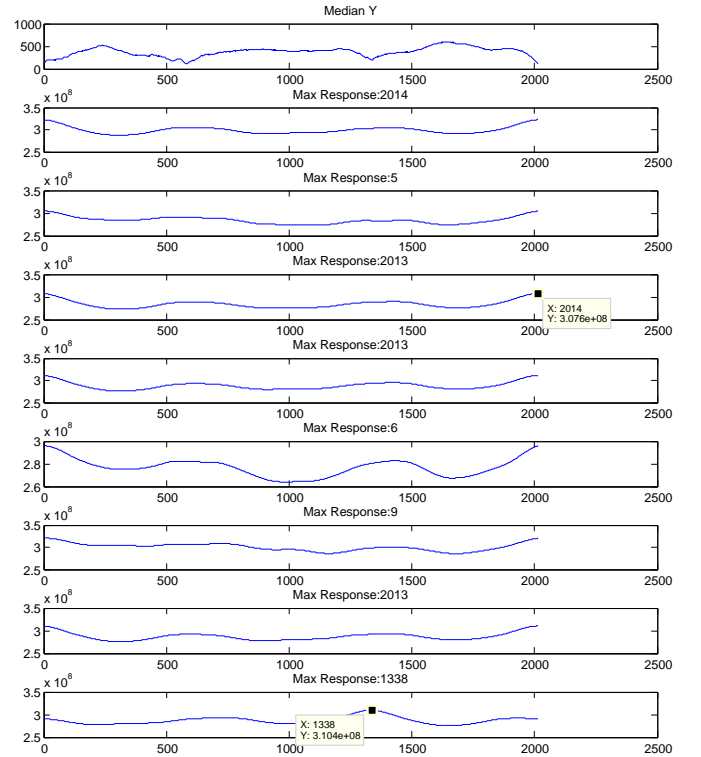
(b) To quatify the similar patterns of the residue energy. We first construct the median residue energy(Median Y) and then calculate the circular correlation between the residue energy and the Median Y. As we can see, when the point clouds are consistently indexed the max response appears near zero (circularly) as respect to frame 01 to 07, but the for frame 08 the max appears at the 1338 which is correspondent to 2676 considering the circulation has a step=2. This is exactly how much the index of frame 08 is shifted from the others.

Figure 4: *Results of experiment on residue correlation*

FISHER, M., RITCHIE, D., SAVVA, M., FUNKHOUSER, T., AND HANRAHAN, P. 2012. Example-based synthesis of 3d object arrangements. *ACM Trans. Graph. 31*, 6 (Nov.), 135:1–135:11.

FISHER, M., SAVVA, M., LI, Y., HANRAHAN, P., AND NIESSNER, M. 2015. Activity-centric scene synthesis for functional 3d scene modeling. *ACM Trans. Graph. 34*, 6 (Oct.), 179:1–179:13.

IZADI, S., KIM, D., HILLIGES, O., MOLYNEAUX, D., NEWCOMBE, R., KOHLI, P., SHOTTON, J., HODGES, S., FREEMAN, D., DAVISON, A., AND FITZGIBBON, A. 2011. Kinectfusion: Real-time 3d reconstruction and interaction using a moving depth camera. In *Proceedings of the 24th Annual ACM Symposium on User Interface Software and Technology*, ACM, New York, NY, USA, UIST '11, 559–568.

JIA, Z., GALLAGHER, A. C., SAXENA, A., AND CHEN, T. 2015. 3d reasoning from blocks to stability. *IEEE Transactions on Pattern Analysis and Machine Intelligence 37*, 5 (May), 905–918.

JIAN, B., AND VEMURI, B. C. 2011. Robust point set registration using gaussian mixture models. *IEEE Transactions on Pattern Analysis and Machine Intelligence 33*, 8 (Aug), 1633–1645.

KRÄHENBÜHL, P., AND KOLTUN, V. 2011. Efficient inference in fully connected crfs with gaussian edge potentials. In *Advances in Neural Information Processing Systems 24*, J. Shawe-Taylor, R. S. Zemel, P. L. Bartlett, F. Pereira, and K. Q. Weinberger, Eds. Curran Associates, Inc., 109–117.

LEVY, B. 2006. Laplace-beltrami eigenfunctions towards an algorithm that "understands" geometry. In *IEEE International Conference on Shape Modeling and Applications 2006 (SMI'06)*, 13–13.

LIU, Z., ZHANG, Y., WU, W., LIU, K., AND SUN, Z. 2015. Model-driven indoor scenes modeling from a single image. In *Graphics Interface Conference*.

MARON, H., DYM, N., KEZURER, I., KOVALSKY, S., AND LIPMAN, Y. 2016. Point registration via efficient convex relaxation. *ACM Trans. Graph. 35*, 4 (July), 73:1–73:12.

MERRELL, P., SCHKUFZA, E., LI, Z., AGRAWALA, M., AND KOLTUN, V. 2011. Interactive furniture layout using interior design guidelines. *ACM Trans. Graph. 30*, 4 (July), 87:1–87:10.

MYRONENKO, A., AND SONG, X. 2010. Point set registration: Coherent point drift. *IEEE Transactions on Pattern Analysis and Machine Intelligence 32*, 12 (Dec), 2262–2275.

NAN, L., XIE, K., AND SHARF, A. 2012. A search-classify approach for cluttered indoor scene understanding. *ACM Trans. Graph. 31*, 6 (Nov.), 137:1–137:10.

NEAL, R. M., AND HINTON, G. E. 1998. *A View of the Em Algorithm that Justifies Incremental, Sparse, and other Variants*. Springer Netherlands, Dordrecht, 355–368.

OVSJANIKOV, M., BEN-CHEN, M., SOLOMON, J., BUTSCHER, A., AND GUIBAS, L. 2012. Functional maps: A flexible representation of maps between shapes. *ACM Trans. Graph. 31*, 4 (July), 30:1–30:11.

PAPON, J., ABRAMOV, A., SCHOELER, M., AND WRGTTER, F. 2013. Voxel cloud connectivity segmentation - supervoxels for point clouds. In *2013 IEEE Conference on Computer Vision and Pattern Recognition*, 2027–2034.

RODOL, E., BUL, S. R., AND CREMERS, D. 2014. Robust region detection via consensus segmentation of deformable shapes. *Computer Graphics Forum 33*, 5, 97–106.

WANG, F., HUANG, Q., AND GUIBAS, L. 2013. Image cosegmentation via consistent functional maps. In *Computer Vision (ICCV), 2013 IEEE International Conference on*, 849–856.

XU, K., CHEN, K., FU, H., SUN, W.-L., AND HU, S.-M. 2013. Sketch2scene: Sketch-based co-retrieval and co-placement of 3d models. *ACM Trans. Graph. 32*, 4 (July), 123:1–123:15.

XU, K., HUANG, H., SHI, Y., LI, H., LONG, P., CAICHEN, J., SUN, W., AND CHEN, B. 2015. Autoscanning for coupled scene reconstruction and proactive object analysis. *ACM Trans. Graph. 34*, 6 (Oct.), 177:1–177:14.